View metadata, citation and similar papers at core.ac.uk
brought to you by CORE
provided by NASA Technical Reports Server

# AVCO LYCOMING QUIET CLEAN GENERAL AVIATION TURBOFAN ENGINE

Craig A. Wilson
Avco Lycoming Division

## SUMMARY

Avco Lycoming participated in the NASA QCGAT program by developing a fan module using an existing turboshaft engine. The fan was designed using the latest in large engine noise control technology. A mixer was added to reduce the already low exhaust gas velocity. A nacelle incorporating sound treatment was provided for the test engine. The noise prediction model was used through the design process to evaluate the various design alternatives. Acoustic tests were then made to verify the prediction and identify the noise characteristics of the fan, core, jet, and sound treatment. Analysis of the recorded data yielded close agreement with the expected results. Core noise, as was expected, was the predominant source of noise for the QCGAT engine. Flyover noise predictions were made which indicated that the Avco Lycoming QCGAT engine would meet the goals set for the QCGAT program.

## INTRODUCTION

The Avco Lycoming Quiet Clean General Aviation Turbofan engine program was designed to demonstrate the latest gas turbine engine noise control technology in a general aviation size engine. A considerable amount of work has been done to identify the design features that offset the generation of noise. And this work is still in progress as can be witnessed by the complexity of the facilities at the Lewis Research Center and elsewhere. The majority of this work, however, has been directed toward the commercial transport class of engines. The QCGAT program was designed to broaden the scope of this effort to include the general aviation size engine. The significant features of the QCGAT design are the low exhaust velocity achieved by a high bypass fan design, the use of a mixer, no inlet guide vanes, subsonic fan blade design, large blade to vane spacing, a high vane to blade ratio, the acoustical lining of the inlet and discharge fan ducts and the use of a long inlet duct. The nacelle and aircraft play an important roll in incorporating these features in the overall acoustic design. For example, the mixer is enclosed in a shroud formed by the nacelle. The fact that forward airspeed mitigates the amount of jet noise

generated has also been factored into the design. These features were optimized for the QCGAT aircraft based upon the results of our prediction of the acoustical performance of the engine aircraft system and the impact of each component on the overall design. The QCGAT noise goals were selected by NASA to force a design that included the latest noise control technology. We responded with an engine design that consisted of adding a new fan design module that incorporated the latest noise techniques of one our turboshaft engines. Our original estimates of the engine noise emissions, based upon that design, are shown in figure 1. Our analysis indicated that the takeoff noise levels would be 4 EPNdB below the goal, the sideline 6 EPNdB below, and the approach 9 EPNdB. This analysis indicated that the core would be the dominant noise source at each measurement position, with the fan contributing to the approach noise and the jet contributing to the takeoff noise levels. Note that the goals are given in terms of aircraft flyover noise. The takeoff measurement point lies 3.5 nautical miles down range from brake release with the aircraft flying directly overhead. The sideline measurement point also lies down range on a takeoff but is displaced 1/4 of a nautical mile to the side and consists of a series of points in order to determine maximum noise level. The approach measurement point is located under the landing flight path at a point 1 nautical mile from the runway threshold. As the approach glide slope is defined as 3° the altitude of the aircraft over the measurement point is 370 feet. Thus we had to consider aircraft performance in the engine design. For this we worked with the Beech Aircraft Co. to define the characteristics of a twin engine QCGAT powered aircraft. With respect to noise, the rate of climb at takeoff, the power required at approach and the geometry of the wing were determined. Airframe noise, however, was not included in our noise estimates.

The design and performance of this aircraft plays an important part in the noise emissions of the QCGAT engines. As has already been discussed, the approach speed and takeoff performance can vary to meet the market requirements of the aircraft. For example, a lower approach power could have been used that would have resulted in lower approach noise levels. As the approach noise levels were predicted to be low, we felt that a small penalty was acceptable to reduce field length requirements. This will allow the aircraft to be certified for use at a large majority of the existing air fields in the United States.

Gas turbine engine noise source identification and control, figure 2, starts with the engine and its geometric and performance characteristics from which prediction of its noise emissions can be made. The engine noise is subdivided into five distinct noise generating mechanisms. They are the fan, compressor, combustionpprocess, power turbines, and the turbulent mixing of the exhaust jet with the ambient air. The majority of

the work done to advance the state-of-the-art gas turbine and aircraft noise identification and prediction was, and is, being carried out by NASA as part of their Aircraft Noise Prediction Procedures (ANOPP), References 1 thru 5. This work has formed the basis of our noise prediction efforts. Of course, we have made certain modifications in order to more accurately reflect our experiences.

These prediction procedures are continuously updated to more accurately predict the engine noise levels. Given the aircraft performance and applying flight effects aircraft flyover noise can be calculated.

## ENGINE DESIGN AND NOISE PREDICTION

The first task was to design a fan module for the engine. This involved several iterations to access the design alternatives. Fan noise reduction was achieved through the use of a low pressure ratio fan to reduce blade loading and noise generation. This has to be part of the fan design from its conception. Other fan design features as shown on figure 3, have also been shown to result in quieter fan designs for the large turbofan engines. Specifically, the fan blade tip speed should be designed to be subsonic. Thus multiple pure tones, or "Buzz Saw Noise" are eliminated altogether. The design relative tip mach number for the QCGAT engine is 1.13 which yields a subsonic value at all sea level operating points. The distance separating the blades from the exit guide vanes should be large when compared to the blade width to reduce rotor stator interaction noise that is expressed in fan broadband noise. We used a value of 2.3 for this ratio. The ratio of fan vanes to blades was optimized at a value of 2.5. This was to eliminate what are known as spinning modes that propagate at the blade passing frequency fundamental. In addition, inlet guide vanes were not used in our fan design. To further insure that inlet turbulence was reduced, a long inlet duct was included in the nacelle design. These features were accounted for in our prediction of the fan noise levels. Our prediction indicated that the fan would be a contributor along with the core only to the approach power levels. By identifying the effect of the various alternatives with the aid of our prediction procedures we were able to maintain this balance to achieve a low noise signature at approach.

An aircraft engine operates differently in flight than it does tied down to a test stand. Its noise characteristics also change. In flight, the air inflow is streamlined due to both flight cleanup affects of the forward air speed and the absence of ground turbulence that influence the generation of fan noise, particularly the tone at the blade passing frequency. Forward flight however, has its greatest impact on the generation of jet noise (see figure 4). It acts to reduce the relative velocity between the exhaust

and the ambient air. This can play an important part in the overall design of the engine aircraft system. For example, the airspeed at takeoff is in part determined by the length of runway availability. A longer takeoff roll would permit a higher takeoff speed. Consequently, the same jet noise level and relative velocity could have been achieved using a higher exhaust velocity.

As the aircraft flies past the observer, the sound varies in both time and spectral content. Dynamic amplification acts to increase the noise level as the aircraft approaches, and reduce the noise levels as it recedes. Then there is the doppler effect that imparts a frequency shift to the noise spectrum as the aircraft flies past. These phenomena must be accounted for to accurately predict the perceived noise of the aircraft.

It is the reduction in jet noise that has the greatest potential for noise reduction.

Jet noise is thus the second major element in the QCGAT engine design. A high bypass fan design is used to reduce the exhaust velocity and therefore reduce the noise generated by the turbulent mixing of a high velocity jet. The jet noise predictions indicated the jet would contribute to the takeoff noise and possibly cause the aircraft engine combination to exceed the limits set by the QCGAT goals at the reduced thrust and altitude condition. The calculations showed that the differences between the core engine and the fan exhaust gas velocities would contribute to this turbulent mixing noise (see figure 5).

A six element mixer was then designed to mix the core engine and fan exhaust gas to yield a single low velocity exhaust jet. The mixer, however, is not entirely free of side effects. Pre and post mixing turbulence can be an additional source of noise that has to be dealt with. These noise sources can be reduced by the addition of a shroud. In our design we provided that shroud by extending the nacelle considerably past the mixer to affect a better mix.

The high bypass fan and mixer were designed to reduce the jet noise component to a noise level below that of the core when forward flight effects cause reduction to occur in the jet noise. That leaves the core noise component. Core noise means the noise generated by the combustion process. The engine compressor and turbine noise were predicted to be above the audible range. Their noise sources do not contribute to the perceived noise of the QCGAT engine and were not considered in the design.

Core noise models have, for the most part, been emperically derived. the ANOPP routine was found to be adequate for our turboshaft engines. This prediction model uses combustor mass flow, temperature rise, and pressure drop as the basis for predicting core noise (see figure 6). Emperical data also suggest a 7 to 10 dB reduction for the turbofan version of this model. Core noise is now recognized as a major source in turbofan engine noise and is the focus of much research. We are working on this both in-house and with NASA. However, we have not included any new core noise control features. Some of the design modifications for emissions may have contributed to higher core noise levels. As our prediction showed from the beginning, the core was going to be a significant contributor to the noise characteristics of the aircraft. Consequently, we felt that further fan and jet noise reduction would have been unwarranted.

It has been long recognized that the fan inlet and discharge ducts of the engine nacelle (see figure 7) offer ideal locations for the installation of sound treatment to absorb the noise generated by the fan. Absorptive material are particularly efficient in absorbing sound energy in the high frequency region where much of the acoustical power radiated by the fan is concentrated. In addition, the sound treatment can be constructed of flight worthy materials that add little weight to the aircraft. Finally, the theory and experience of designing sound treatment panels are sufficiently sophisticated to accurately predict the results that will be achieved by a particular design. Consequently, sound treatment panels were employed for the QCGAT engine nacelle to determine the benefits that would be derived from their incorporation in an aircraft design.

The sound attenuation requirements were determined by comparing the predicted noise levels with the QCGAT program goals. The approach position represented the only point where the fan noise was predicted to contribute to the aircraft noise levels. In addition, the frequency of the blade passing tone at approach is located in the more heavily weighted part of the audible spectrum. Consequently, the approach power point was selected for the design of the sound treatment. At the other positions the fan does not contribute to the aircraft noise levels. The Lockheed California Company was contracted to design the sound treatment for the nacelle. Given the dimensional limitations the nacelle imposed upon the placement of the sound treatment and the engine operating parameters at approach, Lockheed generated a set of design curves from which the sound treatment was designed. These curves were based upon an analytical and emperically derived solution to what are known as the convected wave equations. These equations describe the sound generated by the fan as modes of acoustic energy rotating with and against the fan. This acoustic energy can only propagate under certain boundary conditions. The physical characteristics and operating parameters form these boundary conditions

and determine which modes will propagate. Lockheed performed this analysis and recommended a design. We then took this design to our Nacelle contractor, Avco Aerostructures, for fabrication.

The Lockheed design recommendations are shown in figure 8. Their design was for a single degree of freedom panel for both the inlet and discharge ducts. This design consists of a solid backing plate held 16 mm (5/8 in) off an inner plate perforated to a 5% open area. A honeycomb cell structure material separates the inner and outer plates. The inlet panel is 330 mm (13 in.) long to fill the available space in the inlet duct. The discharge sound treatment consists of a 45.7 mm (18 in.) long panel on the outer duct wall. The inner duct wall formed by the core cowl was not treated. The discharge panel was terminated before the start of the mixer to simplify the design. Otherwise the radiant heat from the mixer would have necessitated the selection of more expensive materials.

The predicted insertion loss for the fan inlet sound treatment panel at the approach and takeoff points are shown in figure 9. The sound treatment as mentioned earlier was designed for the approach condition. At this power setting the peak attenuation is made to coincide with the blade passing frequency. The insertion loss is higher at the takeoff condition due to the increase in air flow through the engine. The blade passing frequency at takeoff is also higher. The result is an attenuation approximately the same as that for the approach condition.

The predicted attenuation for the fan discharge treatment are in figure 10. The duct width between the inner and outer wall makes the treatment more effective even though the inner wall is not treated.

The test nacelle and sound treatment panels were fabricated by Avco Aerostructures in Nashville, Tenn. The test nacelle was designed without the outer skin and to take insert panels in the fan inlet and discharge ducts where ordinarily the sound treatment would have been placed. Two sets of inserts were fabricated. Each was designed to be of one piece to ease removal and installation during testing and to be rigid enough to maintain the desired wall contours. The panels were of sandwich construction with a honeycomb structure separating the inner and outer plates. The thickness of the honeycomb was determined by the Lockheed sound attenuation requirements. One set was fabricated with a solid inner plate, and one set (see figure 11) was fabricated with an inner plate perforated to achieve a 5% open area. This way we could test the engine with and without sound treatment in the nacelle.

The small radius of the inlet and discharge ducts limited to the depth of honeycomb that could be used without warping the cell structure walls.

Plugging the holes was also considered during design. The honeycomb material selected used a small cell pattern in order to be flexible enough to take the curvature. This meant that there would be fewer holes per cell and more holes blocked by the cell walls as the honeycomb was laid over the perforated plate. Fortunately, we were able to use an adhesive that migrated up the cell walls and did not plug holes. The perforated plate was punched to a 6% open area. When the honeycomb was then bonded to it, the open area was reduced to 5%.

The program goals are given in terms of aircraft flyover noise parameters. Experience has shown that when the engine is placed above the wing, the wing serves as a barrier. A barrier attenuation routine was included in the aircraft model to account for this affect. As shown in figure 12, the wing creates a shadow zone that moves along with the aircraft. As only a small fraction of the noise is refracted around the leading and trailing edges of the wing, the forward radiated fan noise will not reach the ground as the shadow zone passes by.

## ACOUSTIC TEST PHASE

The test phase took most of the month of August to complete. The goals of the test program are shown in figure 13. They were to verify the noise predictions through comparison with measured data, determine the noise reduction of the mixer, and determine the effectiveness of the sound treatment panels.

A test plan was prepared to accomplish these goals. The normal method of recording the noise emitted by the engine is to record the sound pressure levels at nineteen locations on an arc 100 feet from the engine. With the microphones located every 10 degrees, a full set of data over an arc of 180 degrees can be obtained. Four power settings corresponding to the operating envelope of the engine were used. In addition to the far field microphones, acoustic probes were placed on the engine to aid in identifying core and mixer components and the noise reduction of the sound treatment. A barrier was also used during part of the testing to aid in isolating the fan inlet and discharge component sound levels.

Three separate engine configurations were used during the acoustic testing of the QCGAT engine. They are a split flow exhaust nozzle configuration called the referee system, the hardwall nacelle in which the test nacelle, mixer, and hardwall fan inlet and discharge panels were used and the soft-wall nacelle in which the hardwall panels were replaced with the sound treatment panels. Each configuration was tested to record the effect on engine noise at four power settings. The QCGAT engine was mounted in a test frame and after a series of tests in our test cells, it was moved to our

free field test site. This site is located close to the plant in an area free of most noise intrusions and where testing will not intrude into the local community.

The engine in the nacelle and test frame were installed on a rotating test stand. This stand is capable of rotating a full 360 degrees. The normal method of testing is to record the noise of the engine on an arc 100 feet from the engine by five microphones placed 10 degrees apart as shown on figure 14. By rotating the engine and repeating the test points, a full 180 degrees of noise can be obtained with some overlapping points. The microphones at the 170 and 180 degree points were in exhaust stream and were not used.

Positions 5 and 6 indicate the orientation of the engine inlet during the barrier test.

One-half inch condenser microphones fitted with wind screens were placed on the ground as used and recommended by NASA. This allows for a simple 6 dB correction to be used when correcting the measured data to free field conditions for comparison with the predicted noise levels. The microphone array is shown in figure 15. The signal conditioning instrumentation are located in the acoustic data acquisition trailer where the data is recorded on magnetic tape for later analysis.

A sample of the engine performance data is given in Table I. At each test point, a complete set of engine performance data was recorded for use in predicting the engine static noise levels for comparison with the measured sound levels.

The ambient pressure, temperature, and relative humidity were also recorded.

Fan noise is composed of tones that are easy to identify near the axes of the engine, but they blend together at the 90 degree locations. The purpose of the barrier then was to isolate the fan inlet noise from the fan discharge noise by physically placing a barrier between them. This was accomplished at the free field test site with the barrier shown on figure 16. The barrier was constructed of a fixed partition 14 feet high by 20 feet long and a movable partition through which the engine inlet protruded. This effectively removed the fan discharge noise from the measurements of the fan inlet noise. By rotating the engine 40 degrees between measurements, data was recorded over an arc of 80 degrees. The movable partition was then pulled out and the engine rotated 180 degrees so that the exhaust protruded through the barrier when it was moved back into position. The fan discharge noise was then recorded without fan inlet noise contributions. Both of these tests were

run at the same four power setting with the hardwall and the softwall nacelles installed on the engine.

The locations of the engine mounted probes are shown on figure 17. Half-inch condenser microphones were located upstream and downstream of the sound treatment to measure the noise reduction across the inlet sound treatment panels. Semi-infinite wave guide probes supplied by NASA were used to sample the acoustic pressure levels in the primary engine exhaust and at the mixer exhaust plane. These probes consisted of 1/4 inch condenser microphones in a sealed tube. A low volume flow of nitrogen at a pressure just above that in the duct provided a gas seal to prevent hot exhaust gas from entering the tube where it could damage the microphone.

These probes were designed to record the acoustic pressure levels at the indicated probe locations. The recorded data will also be used in coherence analysis to determine what part of the noise in the engine is in fact radiated out to the different far field measurement locations.

The split flow nozzle configuration with the semi-infinite wave guide probes installed in the primary exhaust nozzle are shown on figure 18. This configuration was used to obtain baseline d ata for comparison with mixer noise levels.

## DATA ANALYSIS

The data recorded on magnetic tape was then analyzed. Reducing, organizing, and cataloging all this data was a time consuming task. The analysis was straight forward. During the individual test runs, the engine performance was monitored and the relevant ambient and operating parameters recorded. Using these data and the appropriate cycle sheet data, we could predict the expected sound pressure levels. These were then compared point by point, frequency by frequency, and angle by angle with the measured sound pressure levels. In this manner, we estimated the contribution of each component to the overall noise levels at each power setting. The predictions were then adjusted to reflect this comparison, and the correlation was run again. We also evaluated the insertion loss due to the sound treatment and determined the mixer noise reduction.

With the appropriate flight corrections and aircraft performance estimates, we were ready to estimate the flyover noise levels. The individual component contirbution to the overall noise levels were determined on a spectrum basis as shown on figure 19. This plot consists of the one-third octave band sound pressure levels over a frequency range from 25 Hz to 20,000 Hz. The procedure for deriving the flyover noise levels only considers the sound pressure levels from 50 Hz to 10,000 Hz. The pre-

dicted fan noise contribution was overlaid. The calculations correctly located the blade passing tone, its harmonics and the broadband component. The magnitude of the blade passing tone fundamental however was underpredicted. Next, the predicted jet noise component was added as shown on figure 20. As was expected, the jet component does not contribute directly to the noise levels at the low power setting when the predicted core noise component is added to the noise spectrum as shown on figure 21. The predicted spectra matches the measured spectral shape. The agreement however is only fair in the mid-frequency region at the blade passing tone fundamental. This same analy sis was carried out for the softwall and split flow configuration. The analysis was also carried out at each power setting. The high power setting is shown on figure 22. Note that the agreement is only fair across the mid and high frequency regions of the spectrum. The low frequency part of the spectra appear to be in close agreement. Here the jet noise component is predicted to be the predominant source. Based upon this comparison and similar ones at other power settings and configurations, we concluded that the jet noise prediction routine is adequate for the QCGAT program. Consequently, the predicted jet noise levels could be analytically removed from the measured data. The remaining noise levels would then be that composed of the core and fan components. Once the jet component had been removed thd sound power levels attributed to the core were then compared with the predicted core sound power levels as shown in figure 23. Also plotted are the sound power levels derived from the acoustic probes located in the primary exhaust. The probe data are shown more as a confirmation of the slope rather than the sound power levels correctly calculated. These data indicate that the core noise model underpredicts the core noise level by roughly 3 dB. This underprediction appears to be independent of the power setting of the engine. A simple 3 dB correction factor was therefore applied to the core noise prediction procedures. After making this refinement to the core noise model, the predicted-to-measured correlation was then rerun. Figure 24 shows that comparison. The spectral agreement between the measured and predicted data is good over the frequency range of interest. Note that the sound levels in the band containing the tone at blade passing are also in good agreement. This indicates that the core noise contributes across the spectrum. The dominance of the core noise can be seen in figure 25. The noise levels in the discharge quadrant are dominated by the core component to the extent that the fan component is almost entirely masked. The core noise component is present in the forward quadrant. The reduction in the fan noise levels by the sound treatment was hard to discern for this reason. When the core noise component is removed from the one-third octave band containing the blade passing tone, and the resulting blade passing tone is plotted against the angle from the inlet, as shown on figure 26, a fan tone directivity plot is formed. The predicted sound pressure levels at the peak angles are also shown for the inlet and discharge quadrants. The expected

results with the barrier in place come from the prediction procedures. Only when the barrier is in place will the measured data approach these lines which it does as can be seen by the dotted lines. This plot shows how the fan noise contributes to the forward and aft radiated engine noise levels. If an observer were to move past this plot as indicated, the noise levels experienced would first rise and then fall off as the observer moved past. Once past the engine, the noise levels would then rise again as the discharge fan noise reached the observer. This is roughly how the static data was converted to observed flight sound levels. At the high power setting (figure 27) the core noise obscures the aft fan tone from the analysis. A small adjustment was made to the fan noise model from which these data were derived. This adjustment had to do with the effect of relative tip design mach number. With this adjustment, we concluded from the agreement shown here and on the previous figure that the fan noise model is accurately computing the fan noise levels. The sharp dip at the 60 degree point is due to the fact that the data from 0 to 40 degrees were recorded at slightly different power settings than the data from 50 to 90 degrees. The predicted data shows this same dip. We feel this is an artifact of the data acquisition process and is not a characteristic of the fan noise. The individual component contributions appear to be adequately predicted once the noted corrections have been made. Figure 28 shows a final comparison of the measured and predicted overall sound power levels. This plot was generated to verify the accuracy of the prediction techniques for the static case before proceeding to the flyover analysis. The agreement shown here indicates to us that the updated noise prediction model accurately reflects the static noise emissions of the QCGAT engine.

As noted earlier, it was difficult to discern the noise reduction of the sound treatment panels from the far field data. Figure 29 shows the one-third octave band sound pressure levels at the upstream and downstream microphone locations in the inlet. Here the acoustic energy is propagating against the air flow in the inlet duct. The upstream microphone then recorded the inlet noise after it had passed through the treated part of the inlet duct. Figure 30 shows that the expected insertion loss and the insertion loss derived from the test data. These are the values that will be used in the flyover noise estimates. Figure 31 shows that the expected and estimated insertion loss for the fan discharge duct sound treatment panels. The discharge panels had no provision for microphones and were unable to discern a noise reduction from the far field data due to the presence of the core noise. We have assumed that the treatment is functioning properly. The estimated values for the discharge sound treatment panels are shown here.

The jet noise levels were predicted to be low due to the use of a high bypass ratio fan. Figure 32 shows the difference between the noise spectra

of such an engine fitted with the split flow nozzle configuration and with the mixer nacelle configuration. The shaded area represents the static noise reduction of the mixer. Above 250 hertz, the core noise source starts to mask the jet noise and above 1000 hertz, the fan is dominant. When flight effects are added, both the mixed and split flow jet components will drop leaving the mixed flow jet noise levels below the core noise levels. The split flow noise levels would drop and be roughly equal in magnitude to static jet noise levels.

The procedures employed (figure 33) in the QCGAT program to assess the noise emissions of a QCGAT powered aircraft are the Federal Aviation Administration's certification procedures for turbojet powered aircraft (Reference 6). This is a very rigorous method. Basically, the FAA requirements call for measuring the aircraft noise every half second as the aircraft flies over the measurement point. For this analysis, predicted data was substituted for the actual measurements. The demonstration engine performance and the Beech aircraft design were used to compute the individual test point performances. These data were then entered into the prediction procedures. The appropriate flight and wing shielding effects were then applied to the individual component noise predictions. The aircraft noise signature was then derived by combining these into a table of aircraft noise. Then by analytically moving the aircraft noise table past the measurement point, the time history of the flyover could be constructed for each half-second interval. These sound levels were then used to compute the tone corrected perceived noise levels for the flyover event. The maximum tone-corrected perceived noise levels was then found along with the time the aircraft noise is within 10 PNdB of the maximum. From these data, the effective perceived noise level is calculated.

Figure 34 shows the tone corrected perceived noise levels versus time for the approach flyover. The maximum tone-corrected perceived noise level, labeled PNLTM occurs after the aircraft has passed directly overhead. The time the PNLT was within 10 PNdB of the value is 8.5 seconds. This plot also shows that the fan inlet and discharge noise are heard at separate times. The valley between the peaks is caused by the lower sound levels generated at the sideline positions. Wing shielding, the shaded portion, acts to cut the inlet peak off early and makes this valley deeper. The core noise component is heard after the aircraft is past as most of the core noise is in the aft quadrant of the engine. Because of the duration correction, the fan component noise levels are higher and contribute more to the effective perceived noise levels. Figure 35 is the same type of plot showint the takeoff flyover tone-corrected perceived noise level time history. Here the time the noise is within 10 PNdB of the max is much longer. At

the approach condition, the altitude at flyover is 370 feet. For the takeoff condition, it is 2600 feet. Consequently, the time will be considerably longer. The maximum tone-corrected perceived noise level also occurs much later as the sound requires longer to reach the observer and because the dominant noise sources are the core and jet. These components radiate most of their acoustic energy in the rear quadrants and, as such, are not heard until the aircraft is past the observer. Also shown here are the higher noise levels of a split flow nozzle configured aircraft. Here the jet component contributes more to the aircraft noise levels both in magnitude and duration. The duration is increased because the jet noise peaks farther aft than does the core noise. This means that the peak noise occurs later in the flyover. Thus, the addition of the mixer not only reduces the aircraft flyover noise levels, the aircraft noise does not linger as long.

## CONCLUSION

For an aircraft powered by two Avco Lycoming QCGAT engines installed in a nacelle that includes a mixer and fan inlet and discharge sound treatment panels and mounted over the wings, the effective perceived noise levels for the takeoff, sideline, and approach conditions will be 68.4, 7.06, and 77.3 EPNdB, respectively. These noise levels shown in figure 36, are below the limits set by the QCGAT program goals. In the analysis, the effect of several alternative engine configurations on the aircraft noise was assessed. For example, removal of the sound treatment panels would add 2 EPNdB to the approach noise levels and still be below the QCGAT goals. The other positions would not be affected. The noise levels shown here are for the engine that was tested and delivered to NASA . When the iterations are completed for this engine design, the increased thrust of the engine will mean that the aircraft will achieve an altitude of 3600 feet over the takeoff point versus the present 2600 feet. This will result in a 3 EPNdB reduction in the takeoff noise levels and a 1 EPNdB reduction in the sideline noise levels. In this case, the split flow exhaust nozzle configuration would be within 1 EPNdB of the QCGAT goals. Figure 37 shows the Avco Lycoming QCGAT engine effective perceived noise levels plotted against the Federal Aviation Administration's Stage III noise standards and the high technology that used by NASA for the QCGAT program goals. This demonstrates that the technology that has worked for the large engine can be transferred to the general aviation size engine. Consequently, turbofan engine noise emissions should not be a constraint to the growth of the general aviation market.

In summary, (see figure 38) large turbofan noise control technology was successfully applied to a general aviation size engine. The stringent program goals set by NASA forced a design that required the use of a

design that required the use of a quiet fan and integration of the nacelle and aircraft in the engine design. This demonstrates that the QCGAT program goals can be met with the latest noise control techniques without incurring a performance penalty.

## REFERENCES


1. Stone, J. R.: Interim Prediction Method for Jet Noise. NASA TM X-71618, 1974.

2. Huff, R. G.; Clark, B. J.; and Dorsch, R. G.: Interim Prediction Method for Low Frequency Core Engine Noise. NASA TM X-71627, 1974.

3. Heidman, M. F.: Interim Prediction Method for Fan and Compressor Source Noise. NASA TM X-71763, 1975.

4. Dunn, D. G.: Aircraft Noise Source and Contour Estimation. NASA CR-114649, 1973.

5. Gillian, R. E.; et al.: ANOPP Users Manual. July 1978.

6. Federal Aviation Administration Noise STandards, Title 14, Code of Federal Regulation, Chapter I, Part 36.


Table I

### TYPICAL ENGINE PARAMETERS
#### RECORDED DURING NOISE TESTS

| ENGINE PARAMETER | TEST CONDITIONS | |
|---|---|---|
| | LOW POWER SETTING | HIGH POWER SETTING |
| Fan Rotor Speed, rpm | 5376 | 9184 |
| Fan Blade Passing Frequency, Hz | 2150 | 3673 |
| Fan Relative Tip Mach Number | .509 | .89 |
| Fan Airflow, kg/sec(lb/sec) | 14.8(32.6) | 26.3(57.9) |
| Fan Temperature Rise, °C(°F) | 6.7(12) | 15(27) |
| Combustor Airflow, kg/sec(lb/sec) | 1.33(2.95) | 2.37(5.22) |
| Combustor Temperature Rise, °C(°F) | 630(1135) | 878(1580) |
| Jet Exit Velocity, kg/sec(ft/sec) | 106(350) | 194(636) |
| Jet Exit Temperature, °K(°R) | 358(645) | 389(697) |

# QCGAT POWERED AIRCRAFT NOISE GOALS

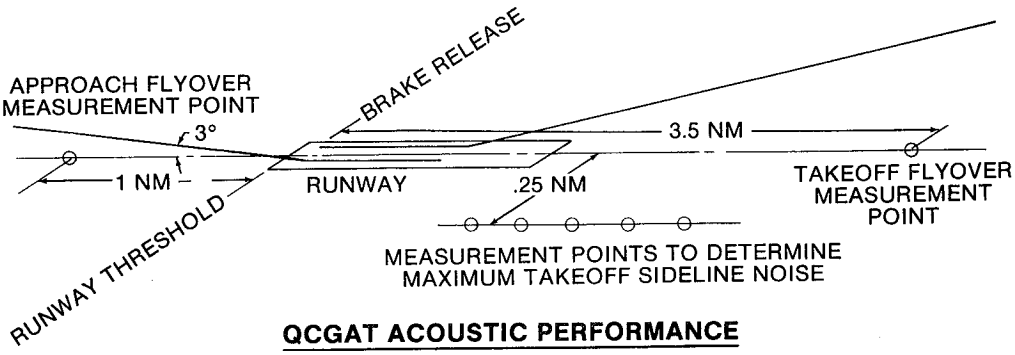


**QCGAT ACOUSTIC PERFORMANCE**

| CONDITION | EPNL GOAL EPNdB | PREDICTED ENGINE EPNL, EPNdB |
|---|---|---|
| Takeoff Flyover | 69.4 | 64.8 |
| Takeoff Sideline | 78.4 | 71.7 |
| Approach Flyover | 83.4 | 73.8 |

Figure 1

# AVCO LYCOMING AIRCRAFT ENGINE

## NOISE PREDICTION PROCEDURES

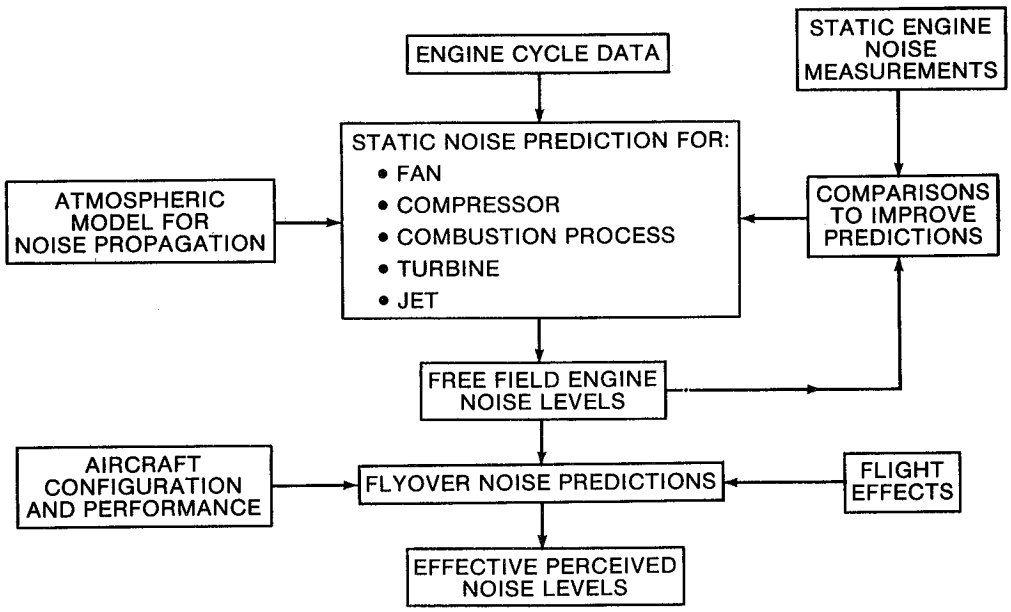


Figure 2

# FAN NOISE REDUCTION TECHNIQUES

| PARAMETER | TECHNIQUE |
|---|---|
| Blade Loading | Low Pressure Ratio |
| Blade Tip Speed | Subsonic |
| Blade to Vane Spacing | Greater Than 2 Blade Widths |
| Vane to Blade Ratio | Greater Than 2 |
| Inlet | No Inlet Guide Vane<br>Low Inlet Turbulence |

Figure 3

# FORWARD FLIGHT EFFECTS

- Reduce Inlet Turbulence
- Reduce Jet Noise
- Dynamic Amplification
- Doppler Shift

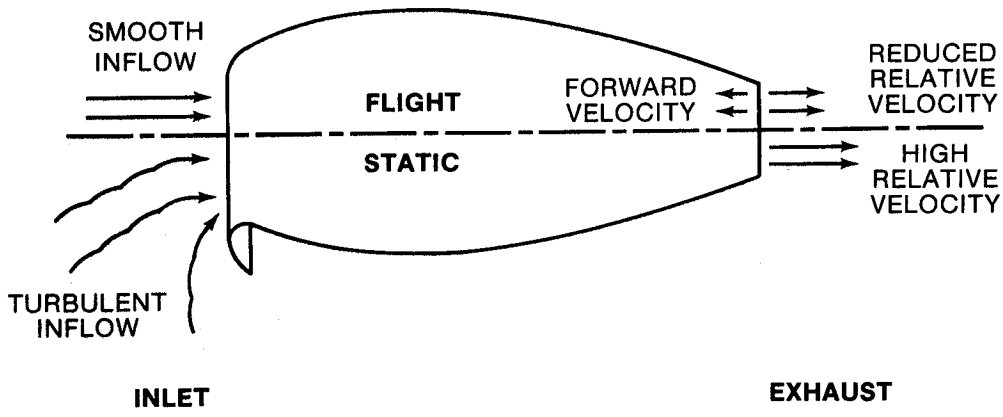


Figure 4

# EFFECT OF NOZZLE CONFIGURATION ON JET NOISE

**WITH HIGH BYPASS FAN**

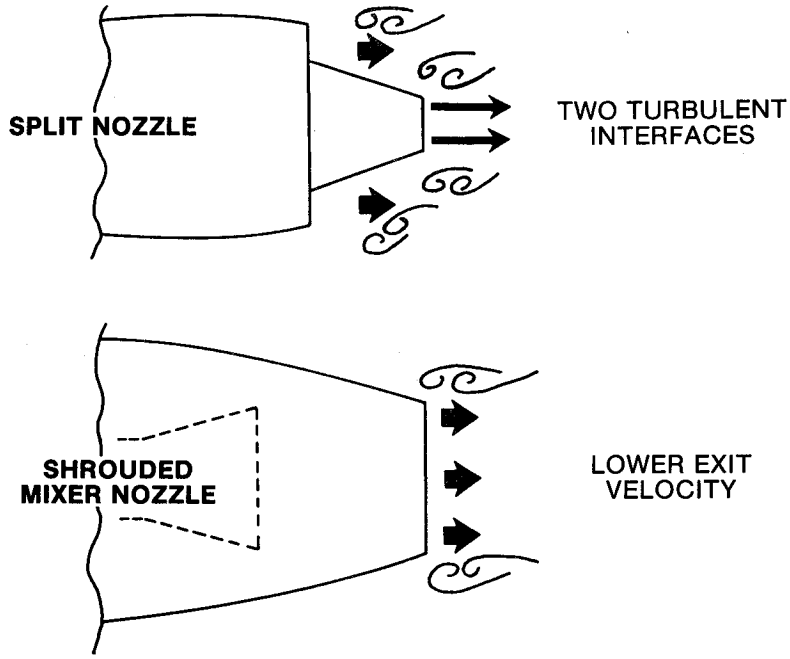


Figure 5

# CORE NOISE MODEL

**(GOOD AGREEMENT FOR TURBOSHAFT ENGINES)**

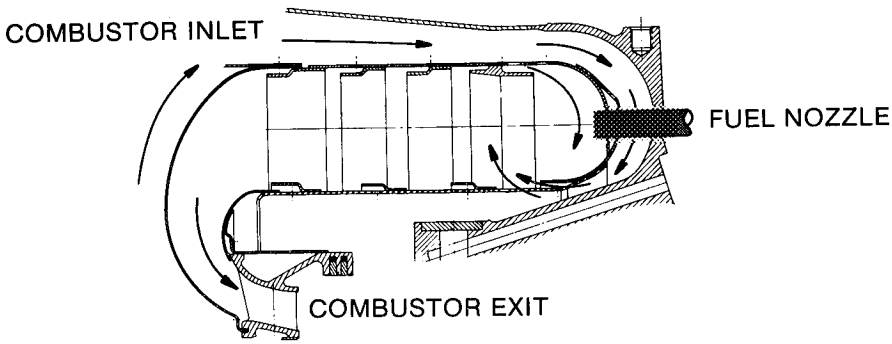


Noise a Function of:

- Mass Flow
- Temperature Rise
- Pressure Drop

Figure 6

# QCGAT FLIGHT NACELLE
# with
# SOUND TREATED PANELS INSTALLED

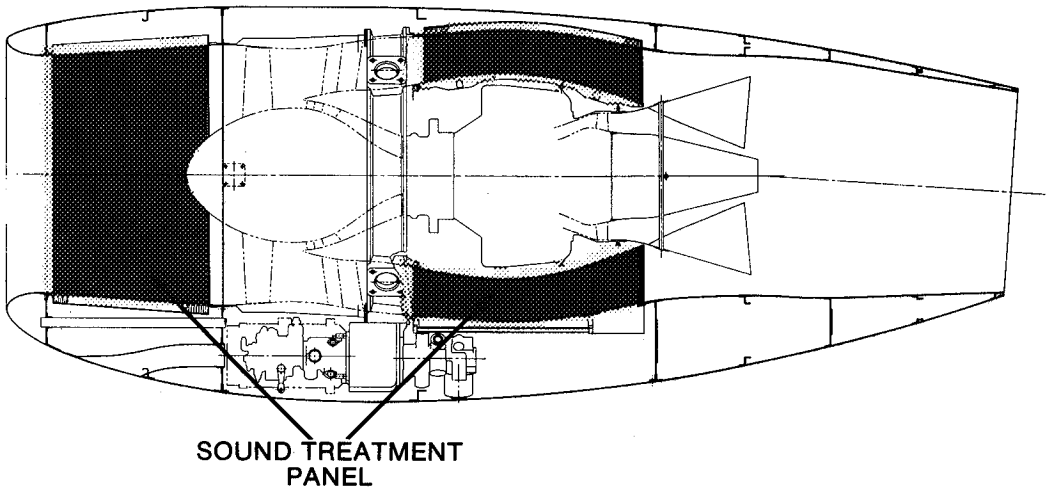


Figure 7

## LOCKHEED DESIGN RECOMMENDATIONS
### FOR SOUND TREATMENT PANELS

| | THICKNESS | LENGTH | OPEN AREA |
|---|---|---|---|
| Fan Inlet | 16mm(0.63 in.) | 330mm(13 in.) | 5% |
| Fan Discharge | 16mm(0.63 in.) | 460mm(18 in.) | 5% |

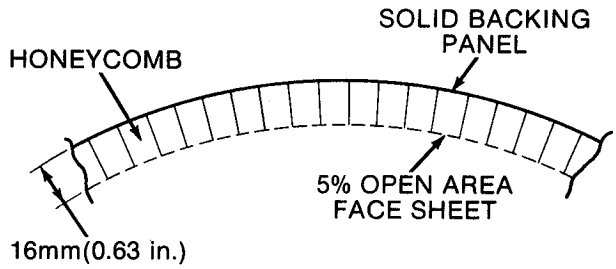


Figure 8

## PREDICTED FAN INLET ATTENUATION

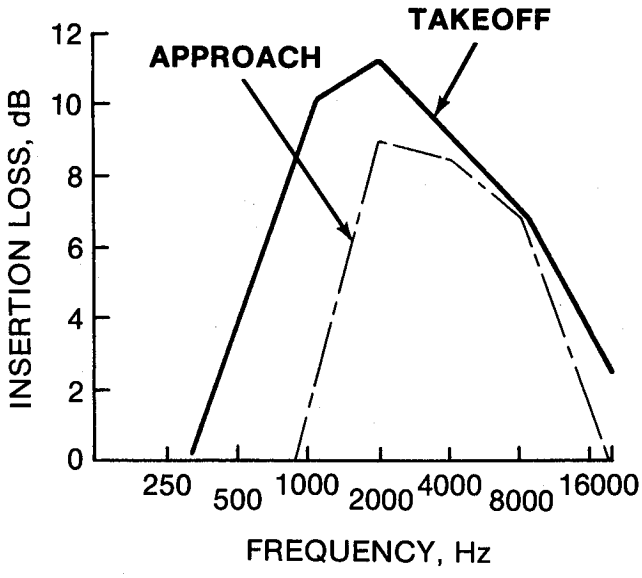


Figure 9

## PREDICTED FAN DISCHARGE ATTENUATION

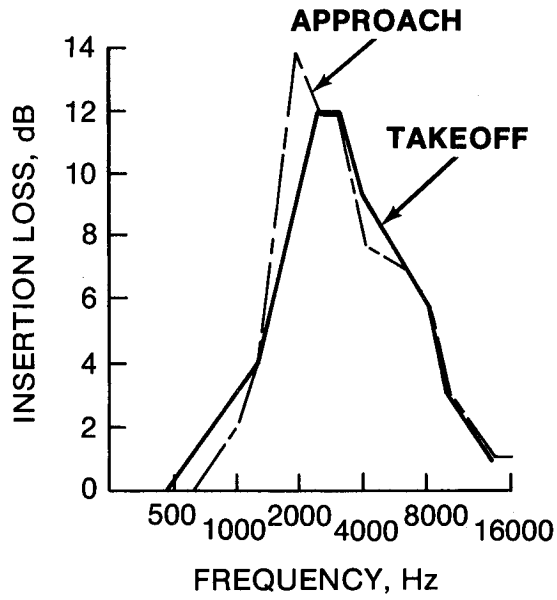


Figure 10

## QCGAT TEST NACELLE

### SOUND TREATMENT PANELS

INLET PANEL

DISCHARGE PANEL

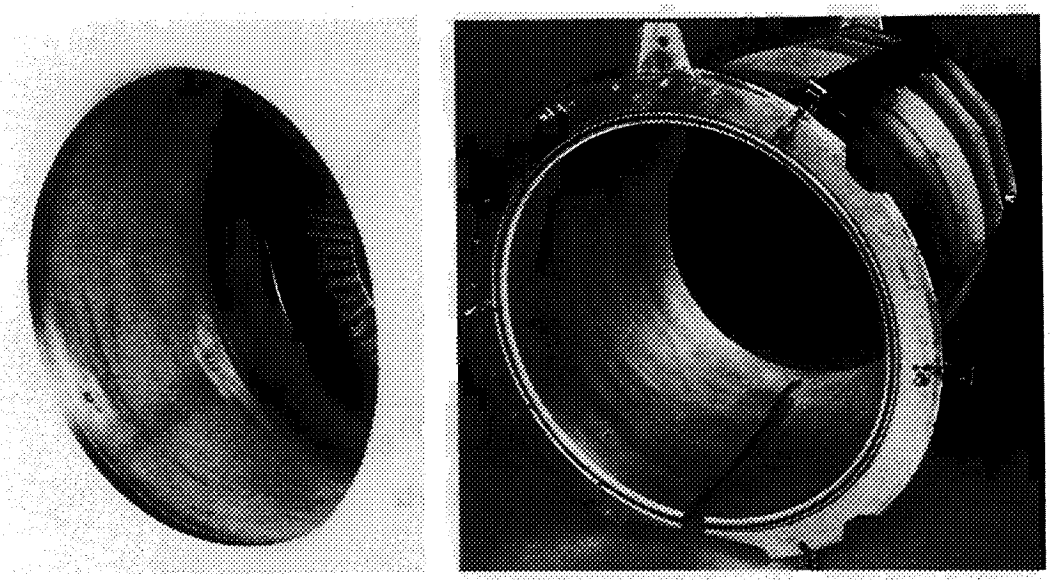

Figure 11

## WING SHIELDING MODEL

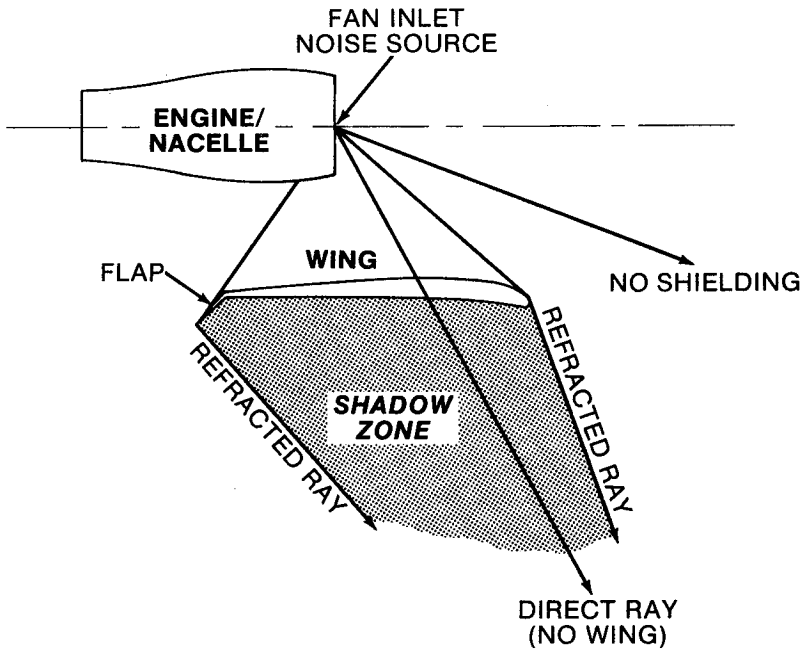


Figure 12

# NOISE TEST PROGRAM

**OBJECTIVES**

- Verify Prediction Procedures
- Evaluate Influence of Mixer
- Determine Effectiveness of Sound Treatment Panels

**NOISE MEASUREMENT (4 Thrust Levels - 180° Arc)**

- Fan Noise - Use Barrier to Isolate Inlet - Discharge Components
- Core and Mixer Noise - Acoustic Probe
- Sound Treatment Panel Effectiveness - Flush Mounted Microphones

Figure 13

# SOUND SITE TEST ARRANGEMENT

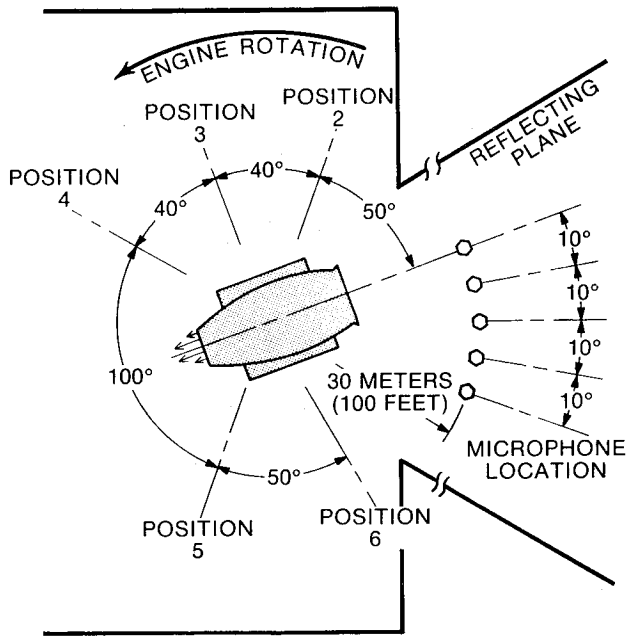


Figure 14

## LYCOMING FREE FIELD TEST SITE

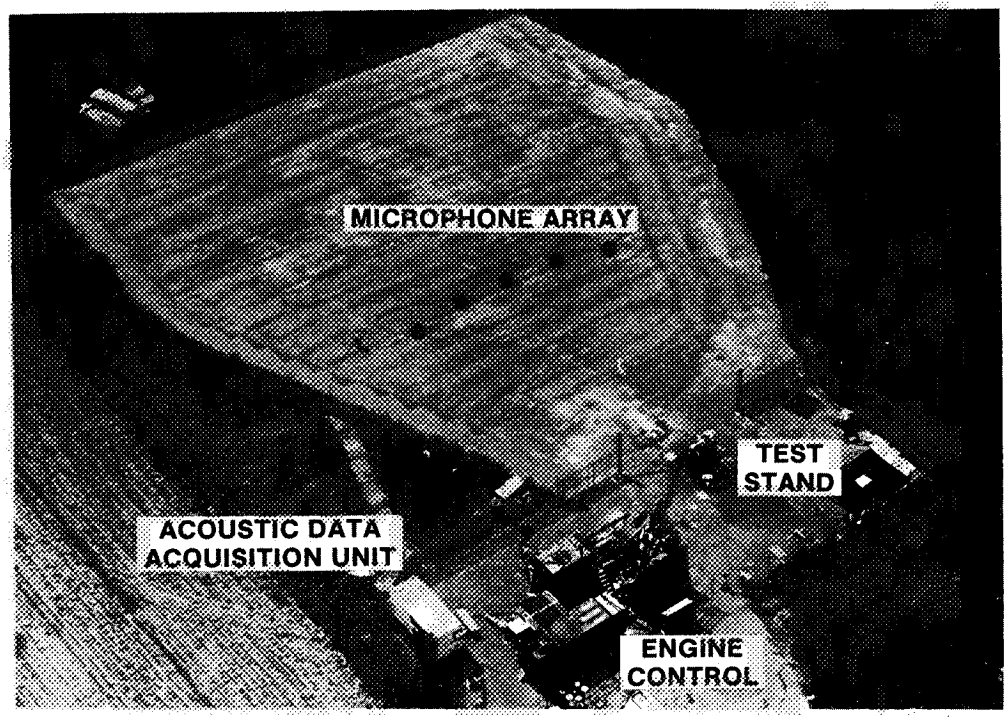


Figure 15

## SOUND ISOLATION BARRIER

### (ISOLATE FORWARD AND AFT RADIATED FAN TONES)

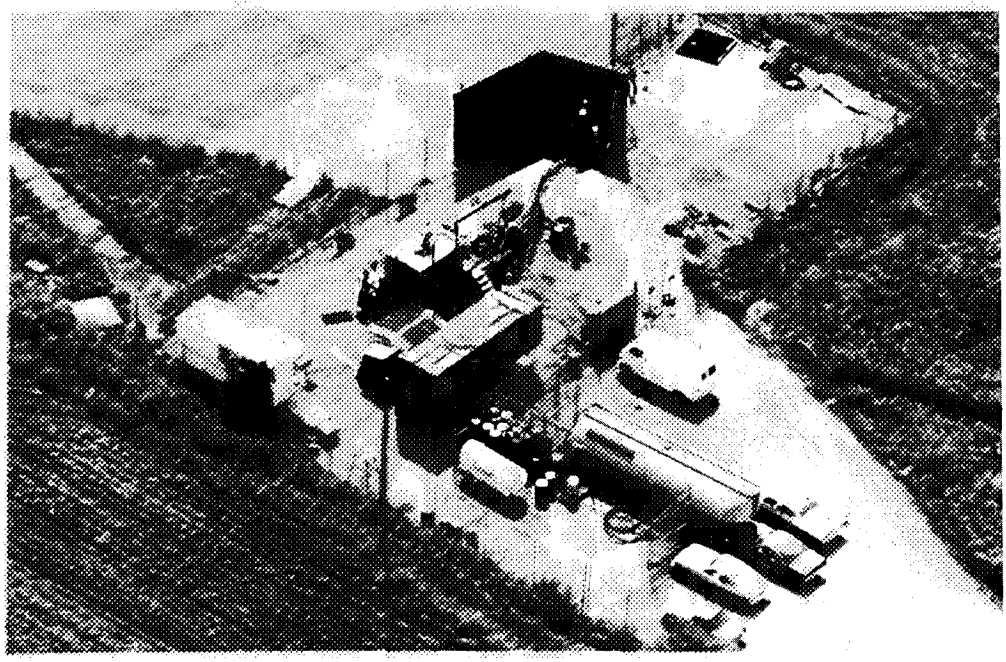

Figure 16

## NEAR FIELD
## ACOUSTIC PROBE LOCATION

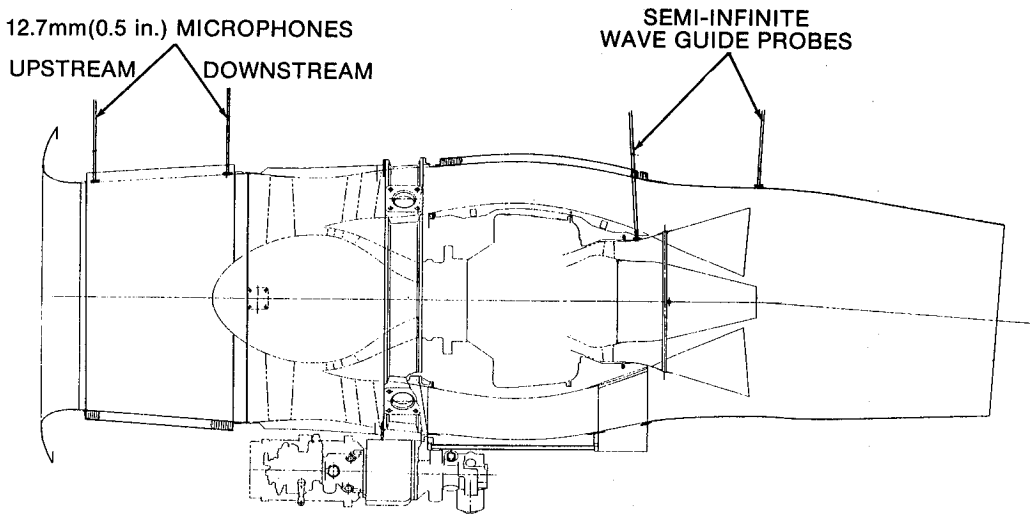


Figure 17

## WAVE GUIDE PROBES
### INSTALLED DURING REFEREE TEST

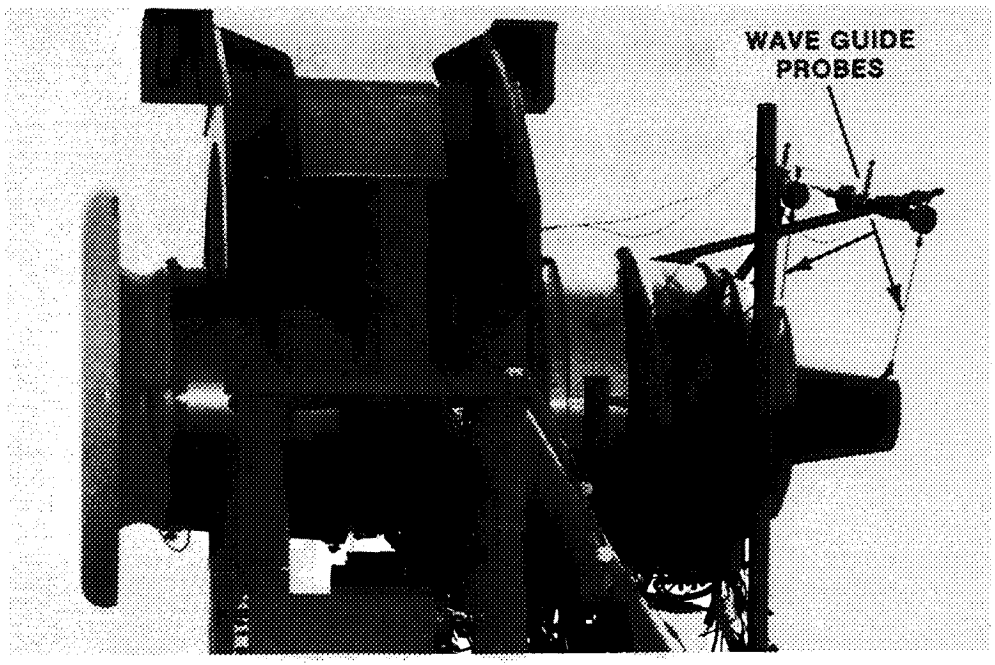


Figure 18

# VERIFICATION OF PREDICTION TECHNIQUES

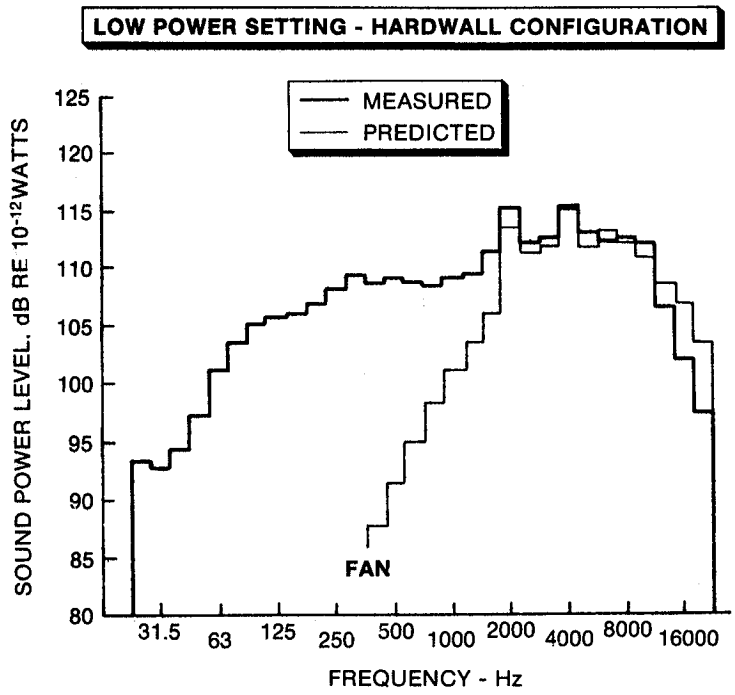


Figure 19

# METHOD OF ANALYSIS

PREDICT STATIC NOISE EMISSIONS AT TEST CONDITIONS

↓

COMPARE WITH MEASURED DATA

↓

DETERMINE COMPONENT CONTRIBUTIONS

↓

REFINE CALCULATIONS TO REFLECT TEST EXPERIENCE

↓

DETERMINE SOUND TREATMENT NOISE REDUCTION

↓

DETERMINE MIXER NOISE REDUCTION

↓

APPLY FLIGHT CORRECTIONS

↓

PREDICT FLYOVER NOISE LEVELS

Figure 20

# VERIFICATION OF PREDICTION TECHNIQUES

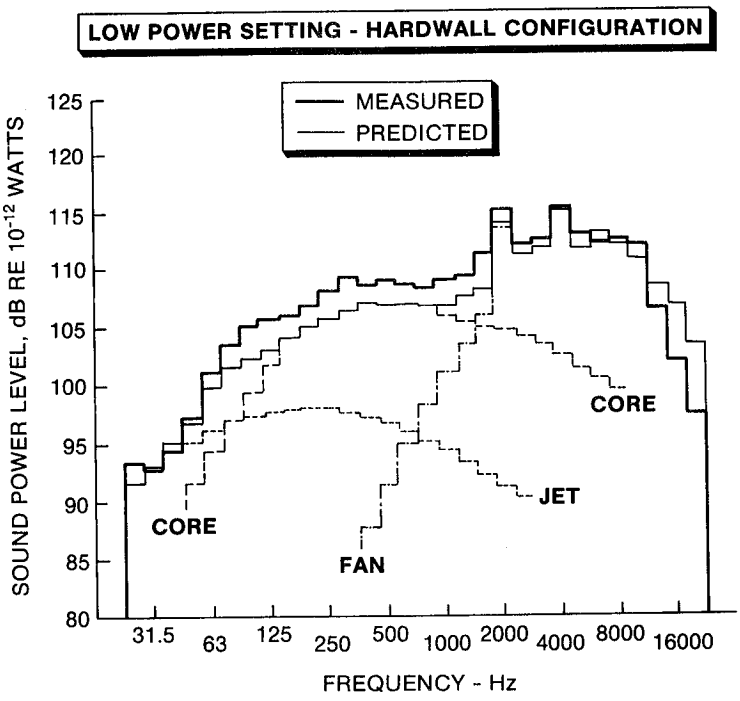


Figure 21

# VERIFICATION OF PREDICTION TECHNIQUES

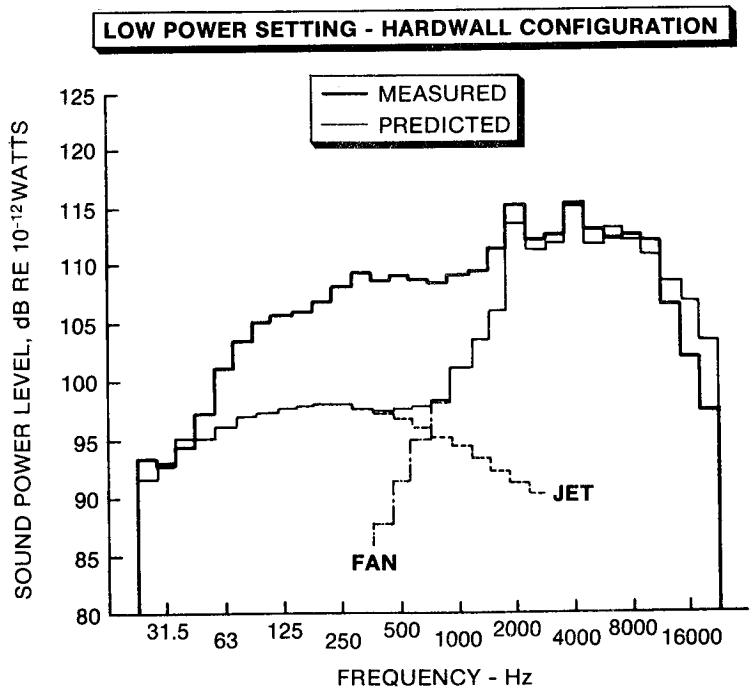


Figure 22

# CORE NOISE PREDICTION

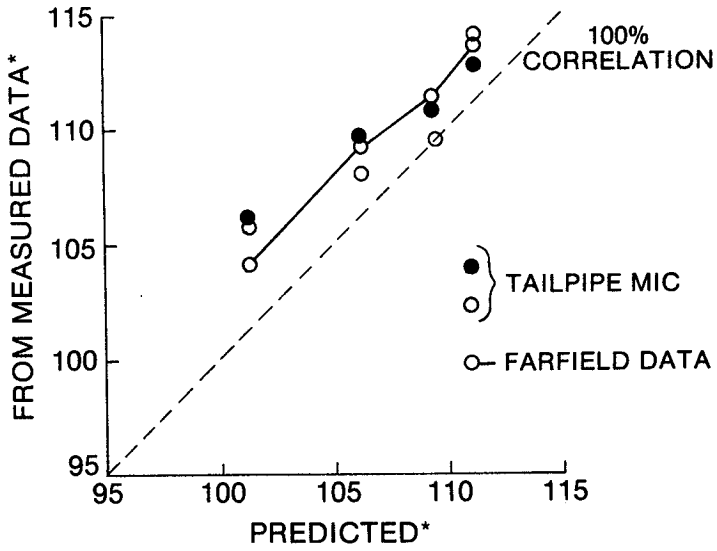


*Sound Power Level, dB RE $10^{-12}$ Watts

Figure 23

# RESULTS WITH UPDATED CORE NOISE MODEL

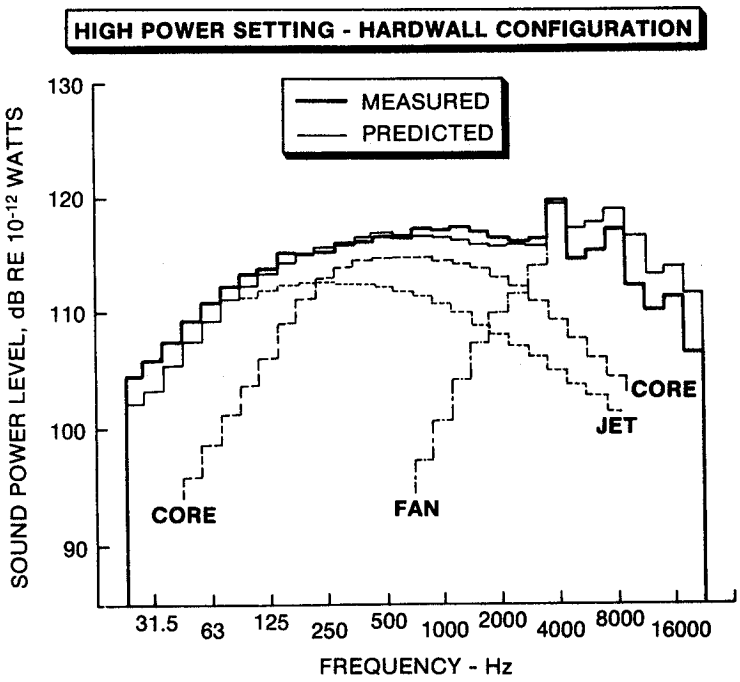


Figure 24

# TYPICAL INLET AND EXHAUST NOISE SPECTRA

- Fan Tone Masked By Core Noise

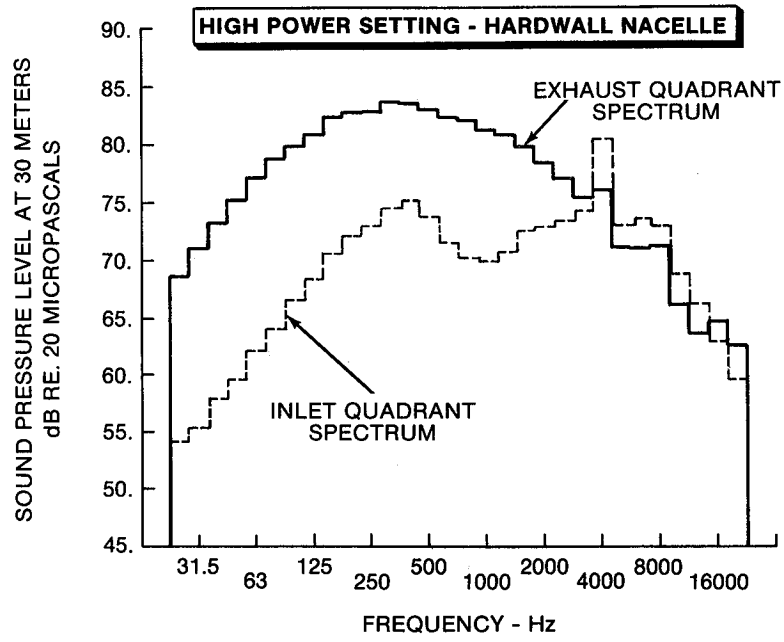


Figure 25

# FAN TONE DIRECTIVITIES

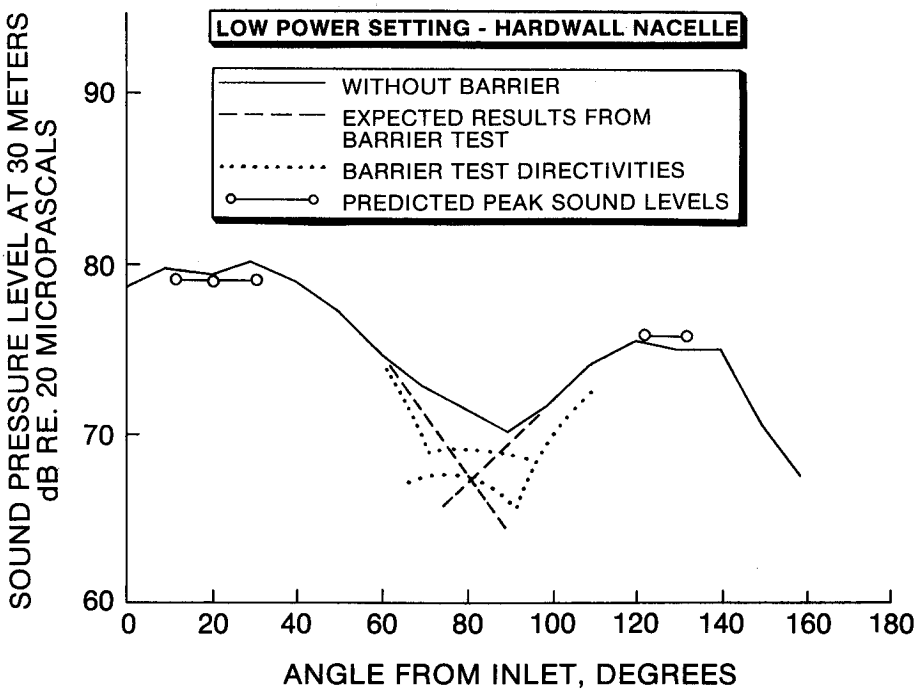


Figure 26

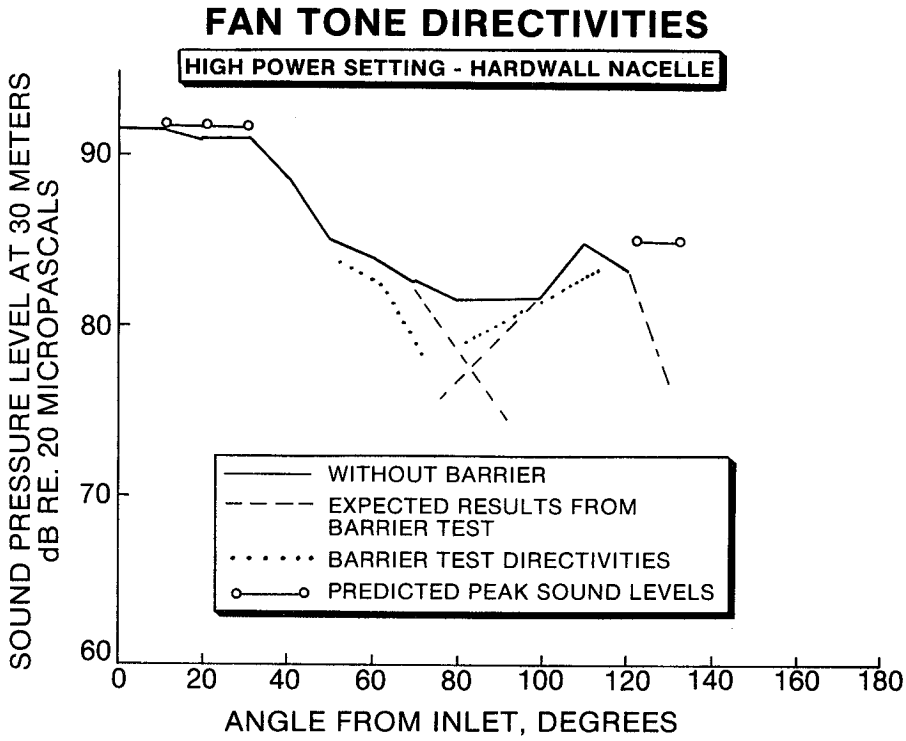


Figure 27

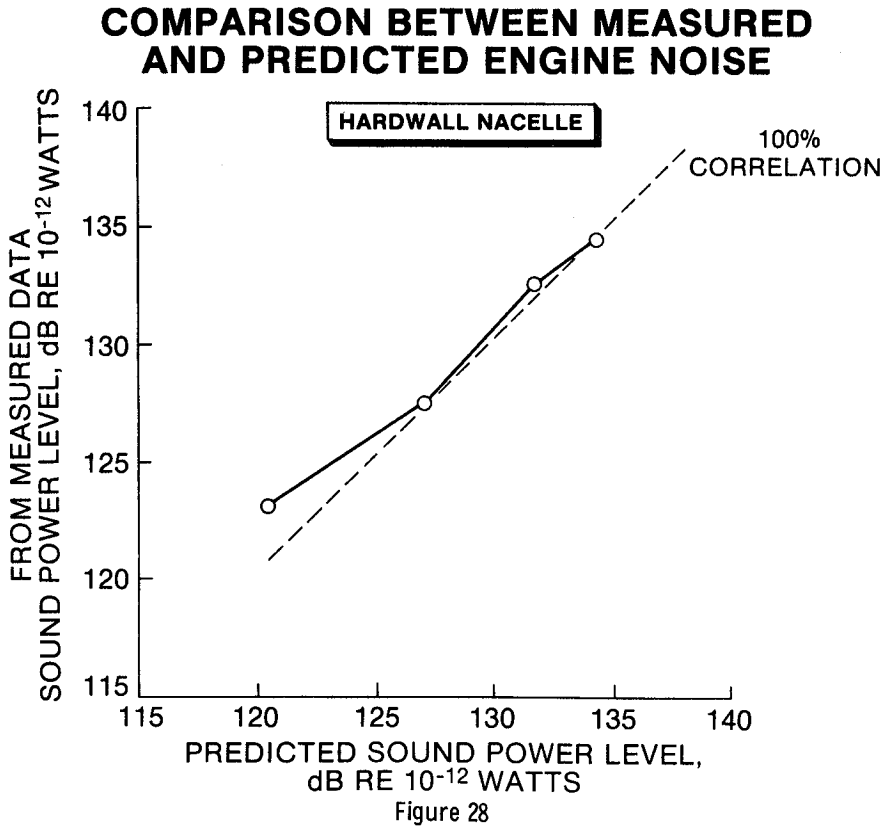


Figure 28

# INLET TREATMENT NOISE REDUCTION

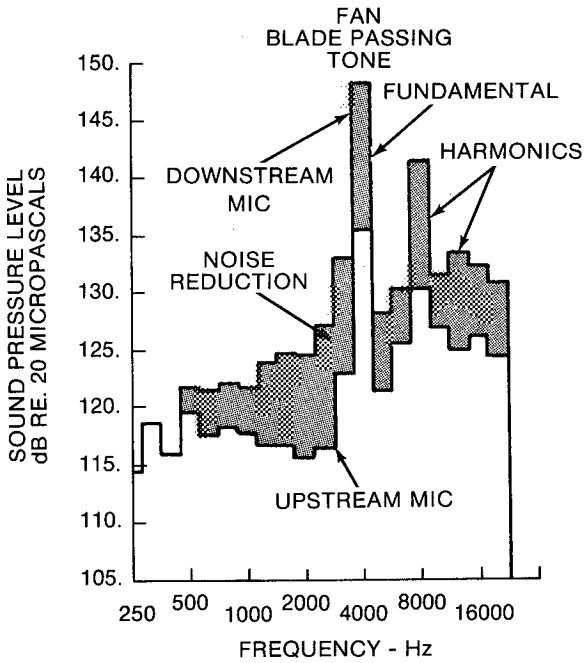


Figure 29

# FAN INLET SOUND TREATMENT

- Treatment Estimated to Meet Design Specifications
- Analysis Limited By Low Fan Sound Levels

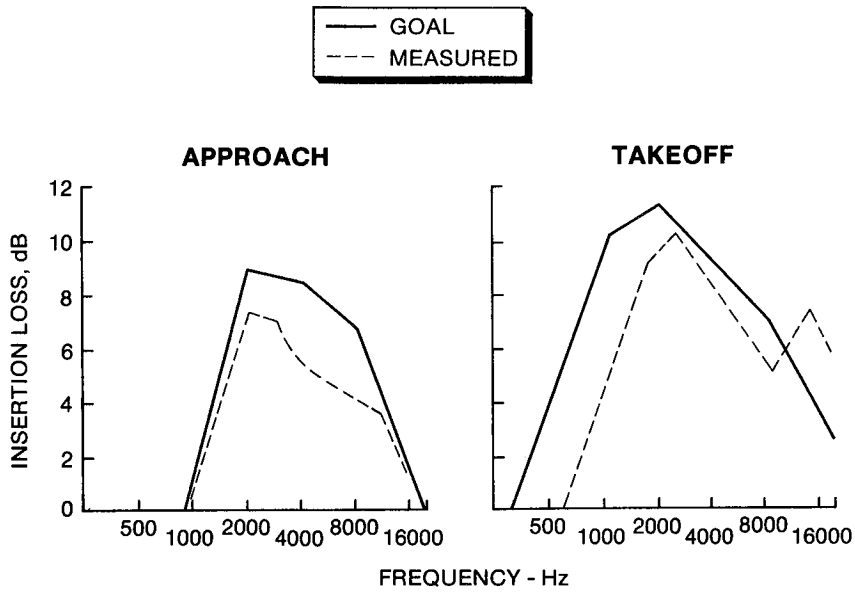


Figure 30

# FAN DISCHARGE SOUND TREATMENT

- Treatment Estimated to Meet Design Specification
- Analysis Limited By Low Fan Sound Levels

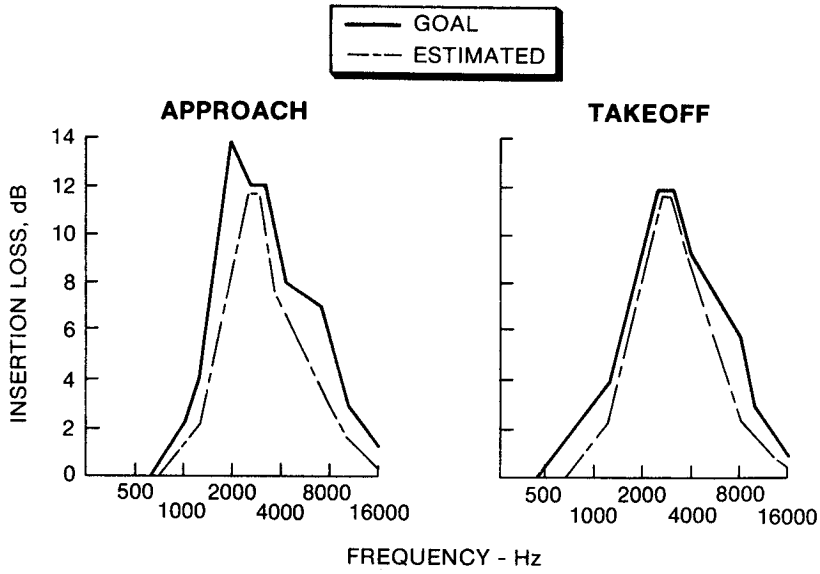


Figure 31

# NOISE REDUCTION DUE TO MIXER

- Greater Than 5 dB
- Coincides with Predicted Results

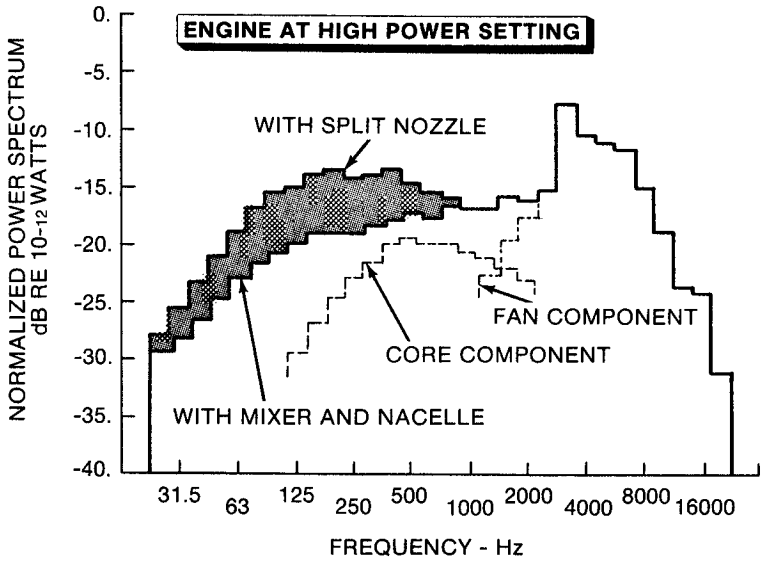


Figure 32

# QCGAT FLYOVER NOISE

## CALCULATION PROCEDURE

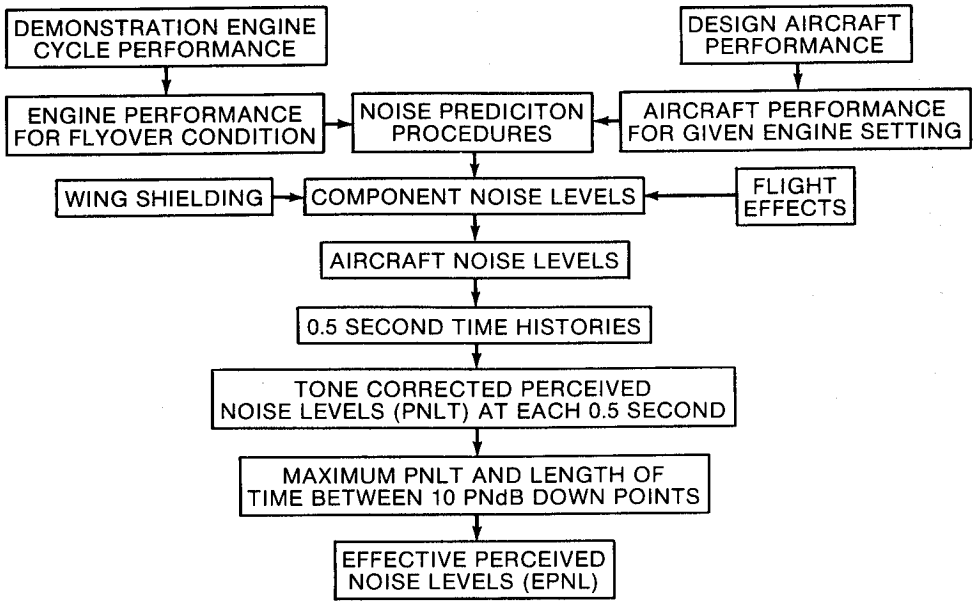


Figure 33

# COMPONENT CONTRIBUTION TO APPROACH NOISE

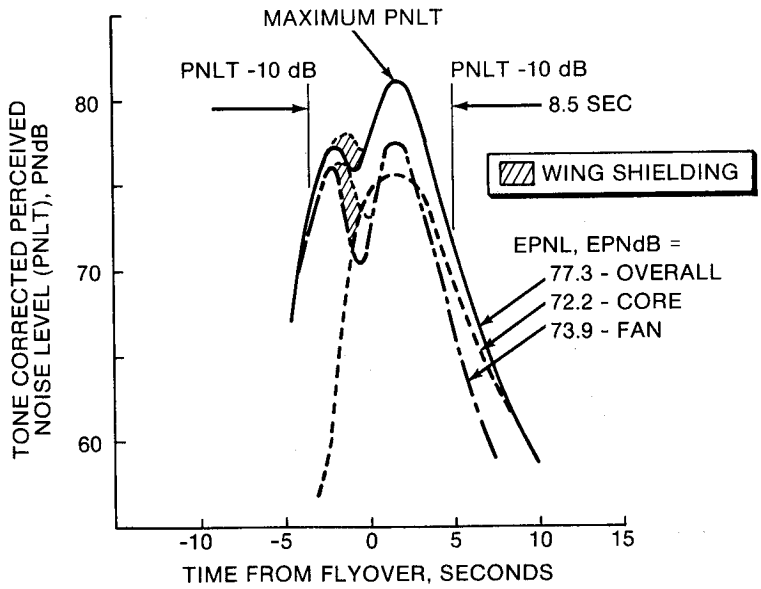


Figure 34

# TAKEOFF FLYOVER NOISE

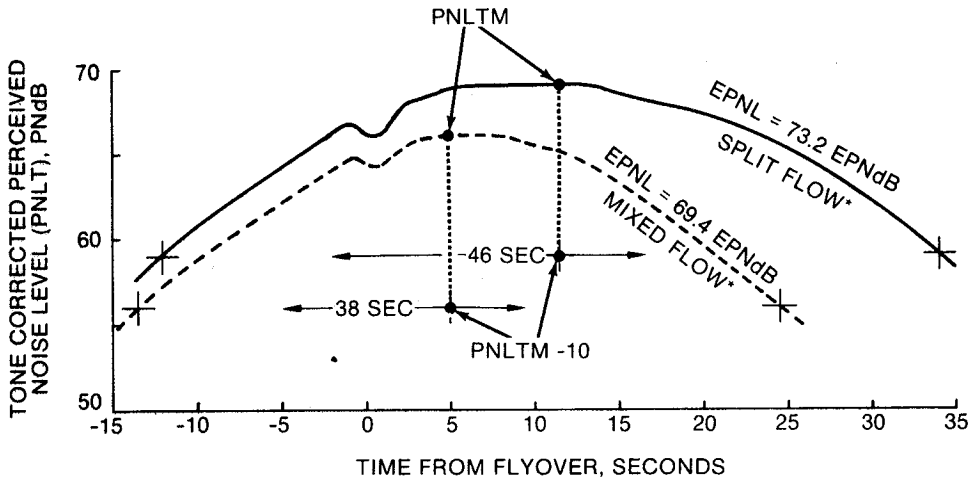


Takeoff Flyover Noise Time History
at Observer Location 3.5 Nautical
Miles Down Range from Brake Release

*No Sound Treatment

Figure 35

# QCGAT PREDICTED NOISE PERFORMANCE

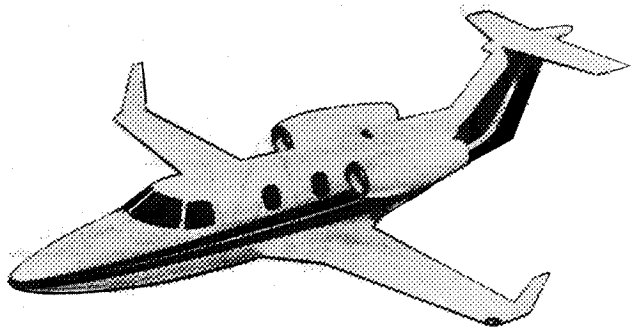

**QCGAT ACOUSTIC PERFORMANCE**

| CONDITION | EPNL GOAL EPNdB | DELIVERED ENGINE EPNL, EPNdB |
|---|---|---|
| Takeoff Flyover | 69.4 | 68.4 |
| Takeoff Sideline | 78.4 | 70.6 |
| Approach Flyover | 83.4 | 77.3 |

Figure 36

## QCGAT vs FAR PART 36 LIMITS

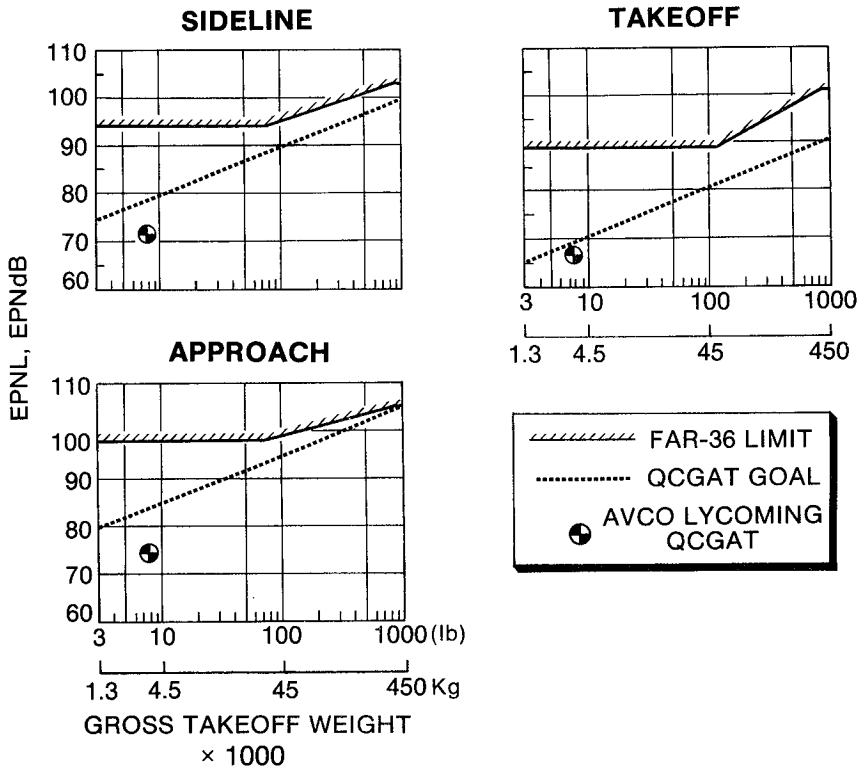


Figure 37

## SUMMARY

- Successful Application of Large Turbofan Noise Control Technology in a General Aviation Size Turbofan Engine
- All QCGAT Noise Goals Demonstrated (Takeoff, Sideline and Approach)
- Used Available Noise Control Techniques to Meet Stringent Noise Goals Without a Performance Penalty
- Noise Need Not Be a Constraint to General Aviation Growth

Figure 38